SOFIA FORCAST Photometry of 12 Extended Green Objects in the Milky Way

Allison P. M. Towner

Ph.D. Candidate

University of Virginia/NRAO

Co-authors: **Crystal Brogan**, Todd Hunter, Claudia Cyganowski, Rachel Friesen

What are EGOs?

Cyganowski et al. (2008) identified in the GLIMPSE survey a class of objects defined by emission extended at 4.5 um but not in other IRAC bands

Size scales of order ~0.1 pc

4.5 um emission is due to shocked H_2 in IRAC Band 2 (e.g. Marston et al. 2004)

Preferentially coincident with IRDCs

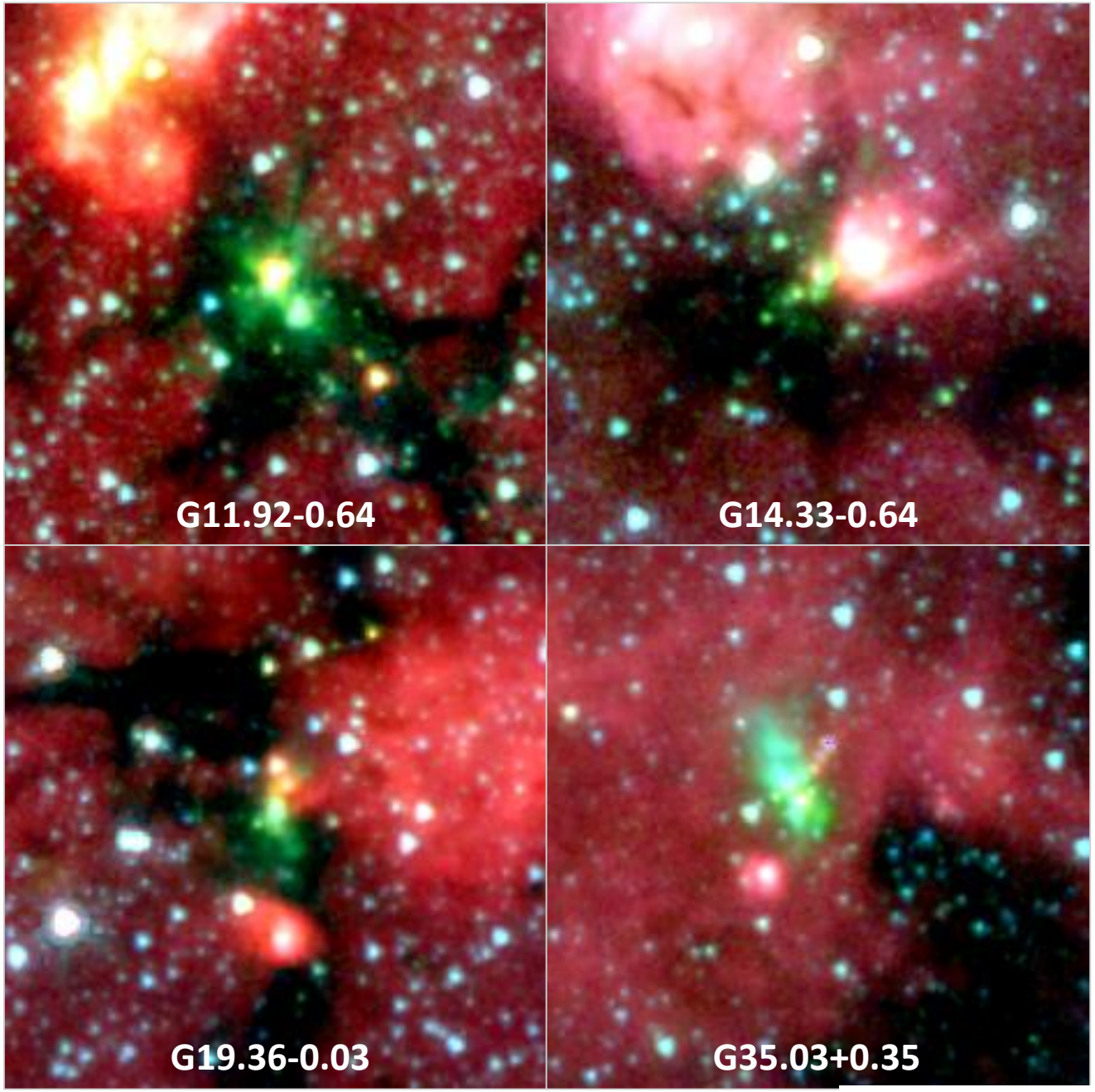

What are EGOs?

Follow-up observations of curated sub-samples identified evidence of:

- outflows (Class I CH_3OH and H_2O masers; Cyganowski et al. 2009, 2013; Towner et al. 2017)

- massive protostars (Class II CH_3OH masers; Cyganowski et al. 2009)

- cold, dense gas (NH_3 (1,1) – (3,3); Cyganowski et al. 2013)

Little evidence of significant ionizing radiation (weak 1.3 cm continuum emission; Towner et al. 2017)

→ EGOs are MYSOs in an active accretion state prior to the emergence of significant ionizing radiation

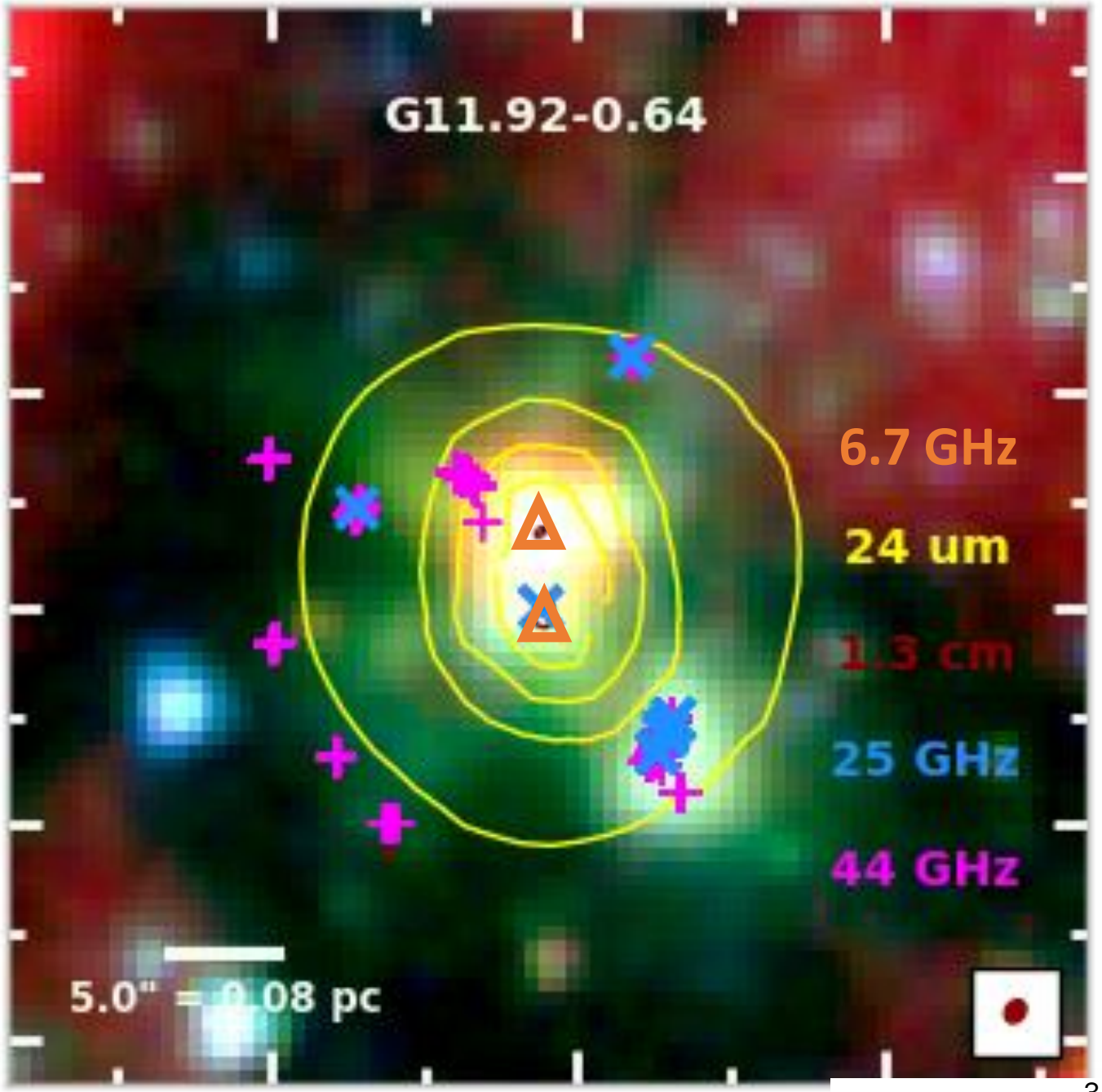

EGO-12 Sample

- 12 nearest, youngest-appearing EGOs from the previous sample: near-IR (3.6 um) to radio (5 cm) observations using archival infrared data, SOFIA, ALMA, and JVLA

- Open questions:
  - Bolometric luminosity
  - Properties of individual cluster members (mass, accretion disk/rate, etc.)
  - Luminosity-to-mass ratio (L/M) of the clump
  - Clustering and multiplicity
  - Birth order
  - Emergence and effect of ionizing radiation
  - Mechanical energy from outflows

EGO-12 Sample: Infrared Observations

- *SOFIA* FORCAST observations: 19.7 um and 37.1 um, ~10 minutes TOS
- Archival observations:
  - *Spitzer* IRAC (GLIMPSE): 3.6, 4.5, 5.8, 8.0 um
  - *Spitzer* MIPS (MIPSGAL): 24 um
  - *Herschel* PACS (Hi-GAL): 70 um and 160 um
  - APEX LABOCA (ATLASGAL): 870 um
- Additional single-dish observations of NH_3 from Cyganowski et al. (2013)
- Project goals:
  - Multiplicity and properties of massive sources
  - Bolometric luminosity
  - Overall clump properties (T, M)
  - L/M as a tracer of evolutionary state of the clump

EGO-12 Sample: Infrared Observations

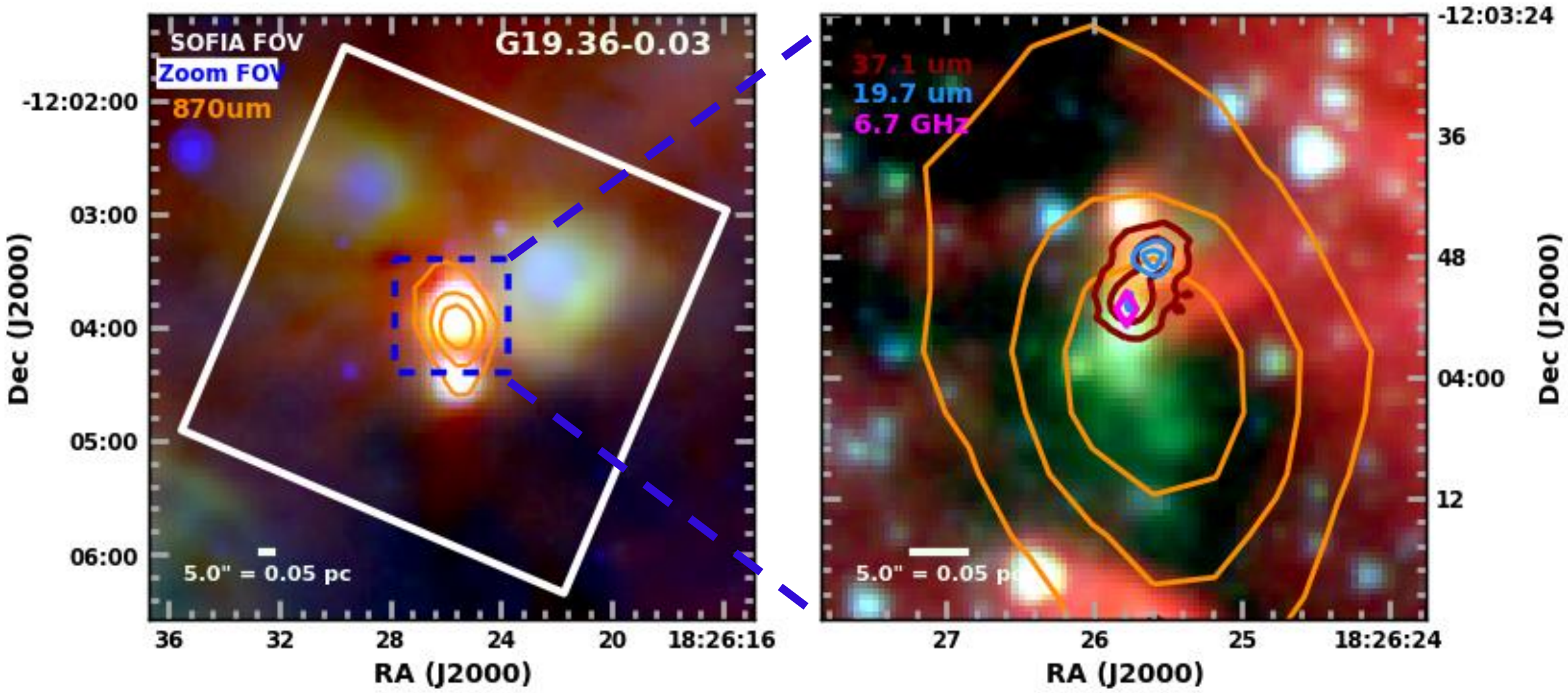

Left: RGB: 160, 70, and 24 um; orange contours: 870 um; white box: SOFIA FOV; blue box: FOV of right-hand panel

Right: RGB: 8, 4.5, 3.6 um; red and blue contours: 37.1 and 19.7 um, respectively; pink diamond: 6.7 GHz

EGO-12 Sample: Multiplicity

Average 37.1 um detections of EGO-associated sources: 2 per FOV

If all 37.1 um detections are truly associated, sample multiplicity of massive sources is 1.9

If only half are, sample multiplicity of massive sources is 1.4

- similar to massive-source multiplicity in a subset of the SOMA sample (Rosero et al. 2019) at this resolution

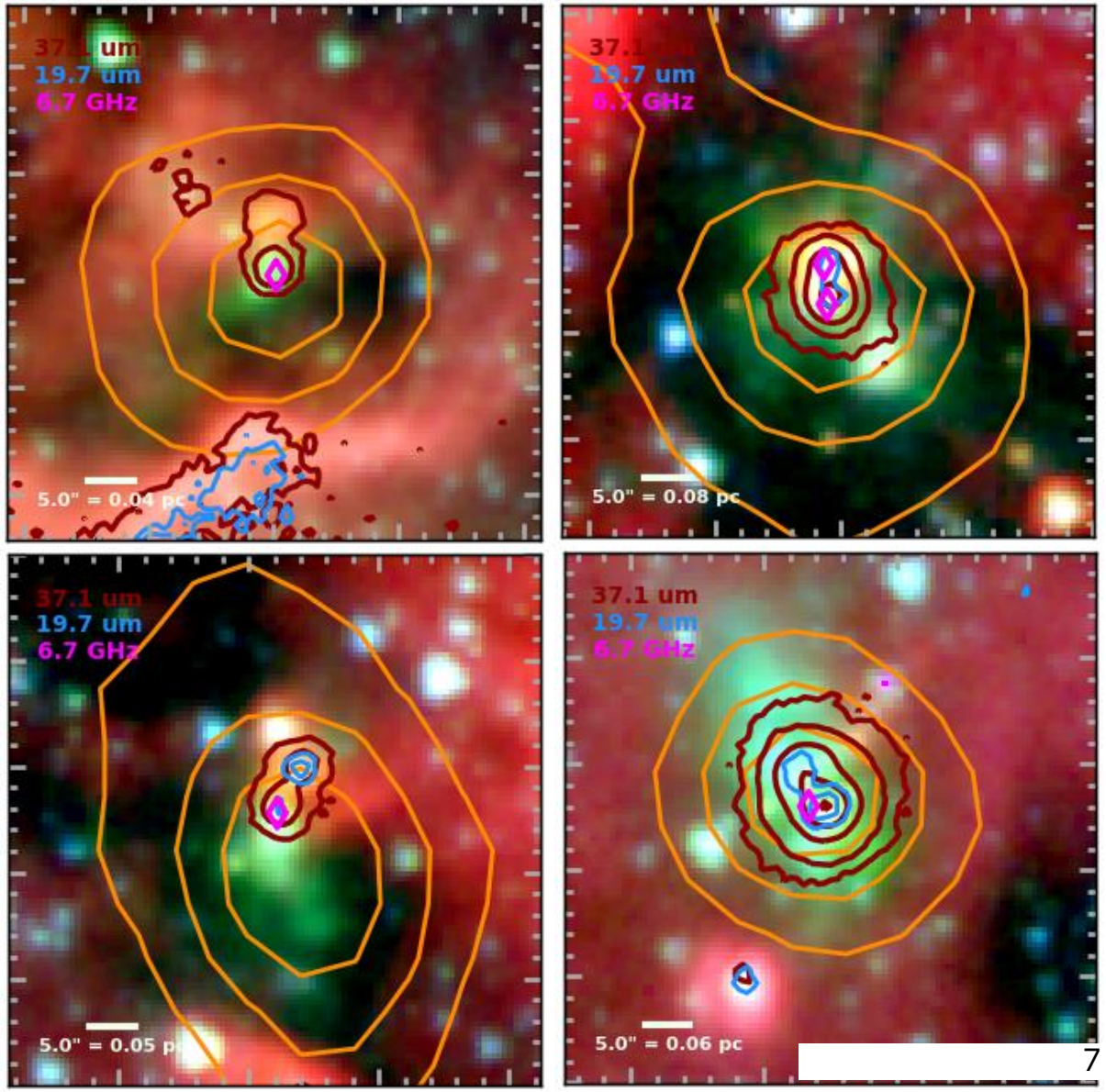

EGO-12 Sample: Luminosities

- To get L_{bol}, we ran graybody fits (via lmfit), plus Robitaille et al. (2006), Robitaille (2017), Zhang & Tan (2018) radiative-transfer models
- L_{gray} is returned directly by lmfit; Stefan-Boltzmann L_{SB} calculated from R and T results for the radiative-transfer models
- $L_{gray} < L_{SB}$ in almost all cases, as expected

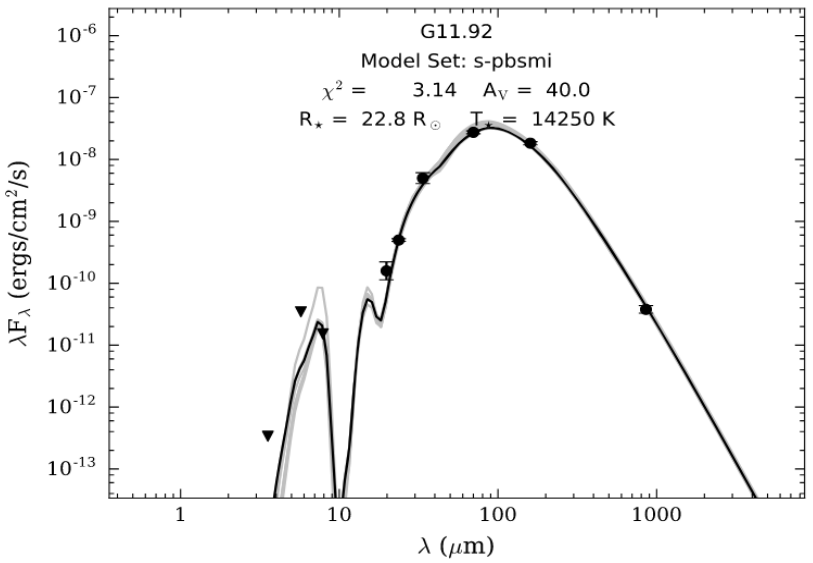

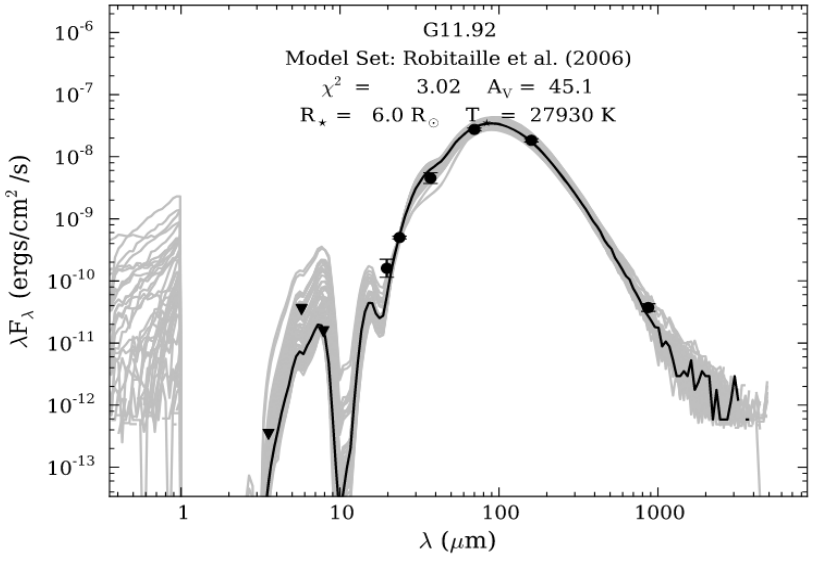

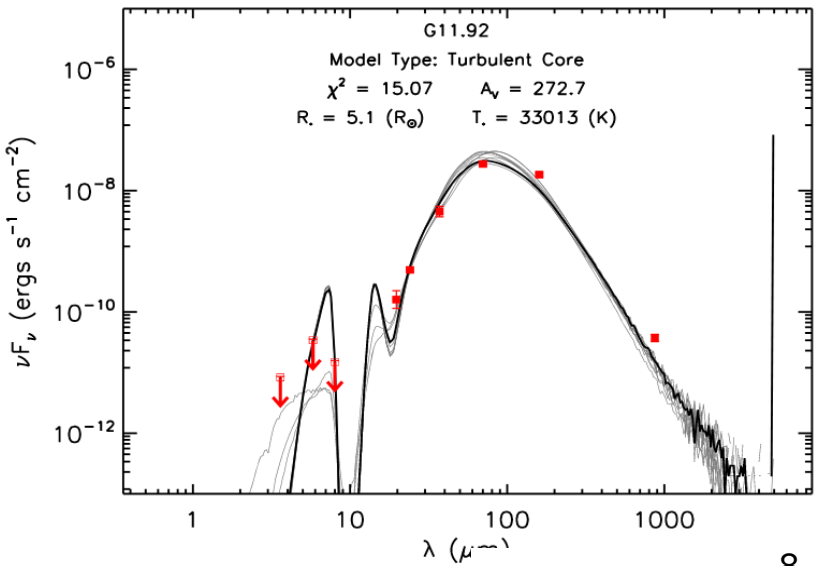

SEDs, left to right:

1. Robitaille (2017)
2. Robitaille et al. (2006)
3. Zhang & Tan (2018)

Notable variation between and among radiative-transfer model results in both SED shape and returned physical parameters

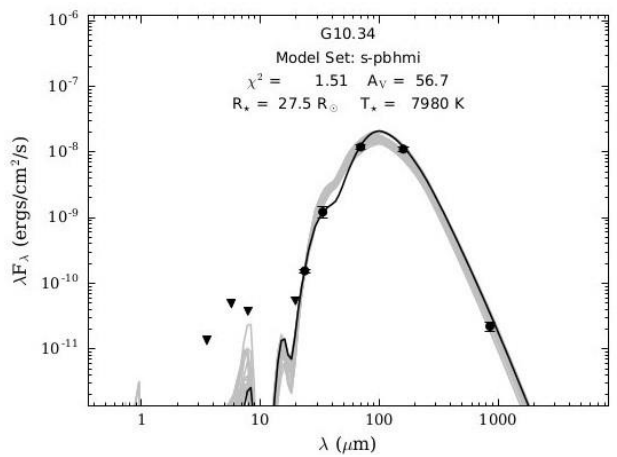

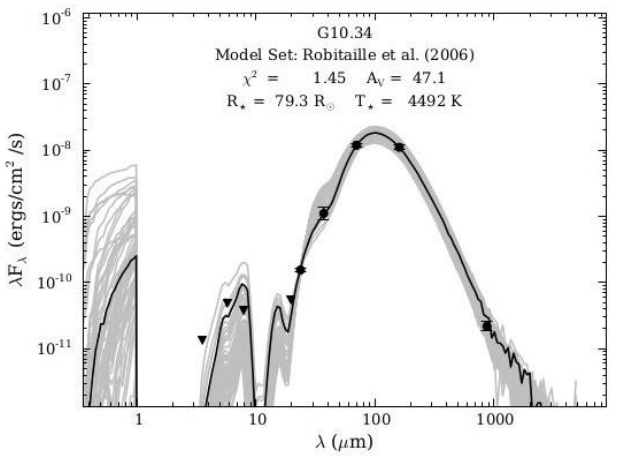

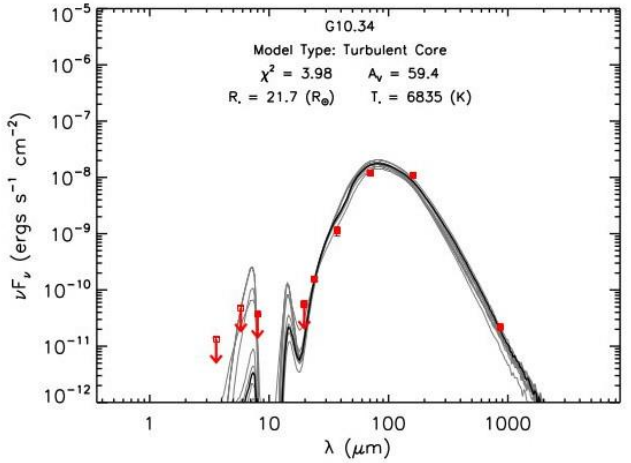

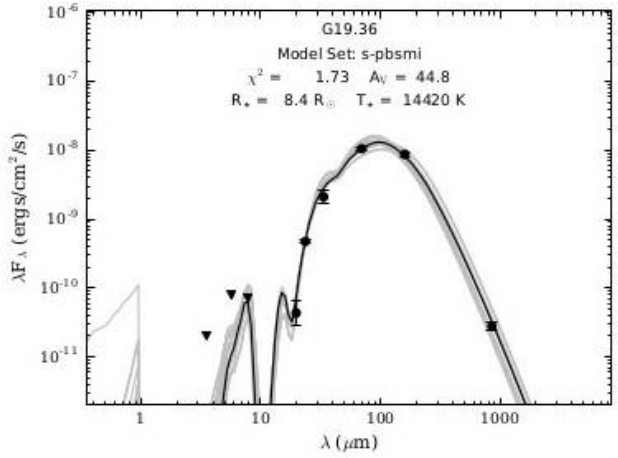

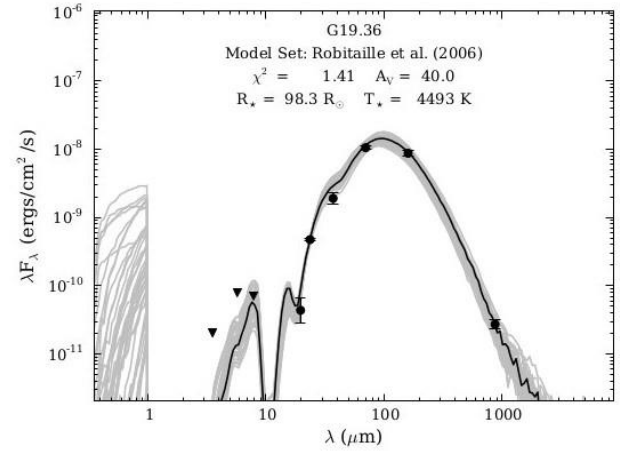

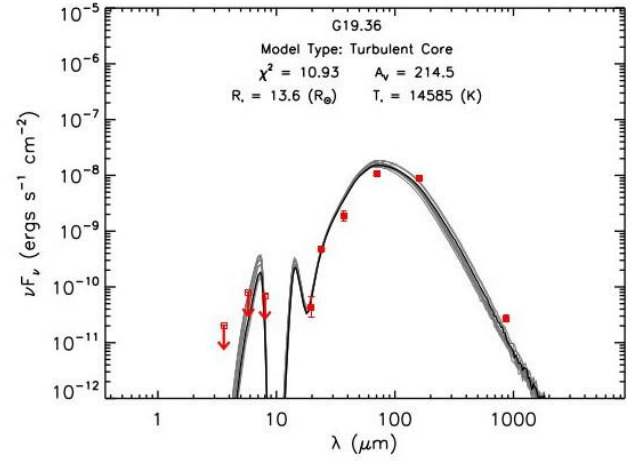

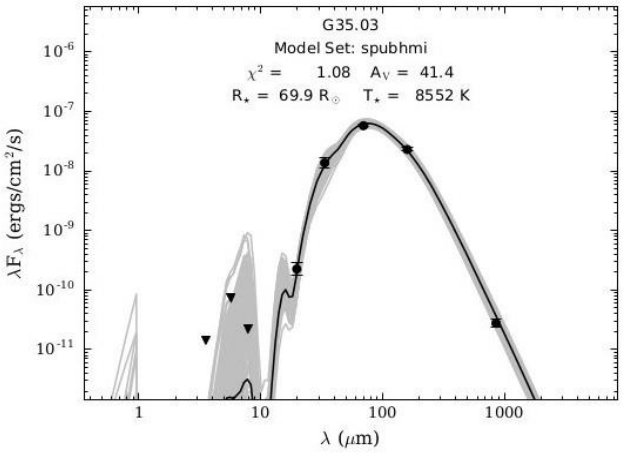

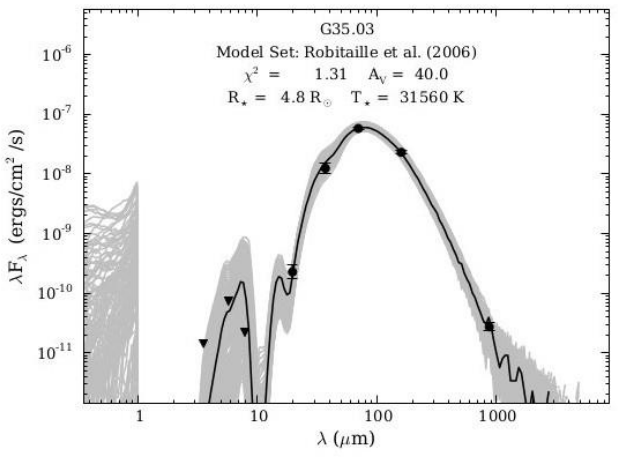

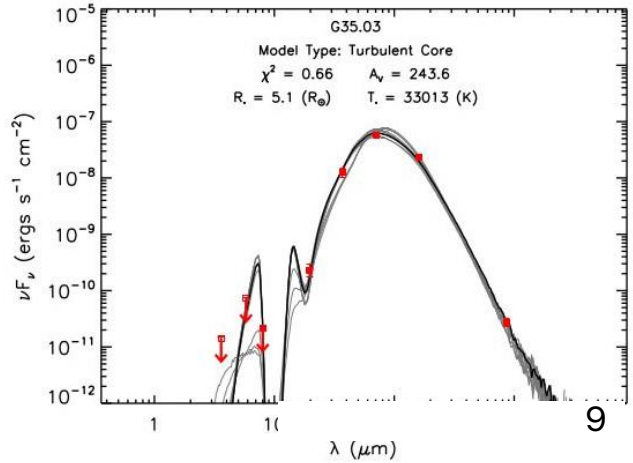

EGO-12 Sample: Trends in Model Results

Stellar radii for a particular source typically span 1-2 orders of magnitude across all three model results (results for G14.33-0.64, right)

Stellar temperatures typically span 1 order of magnitude

Stefan-Boltzmann luminosity typically agrees within a factor of 2.5 across all three results

	Robitaille (2017)[a,b]			
Source	$R_\star$ ($R_\odot$)	$T_\star$ (K)	$L_\star$ (10^3 $L_\odot$)	χ^2
G14.33-0.64	31.4	7976	3.53	0.45

	Zhang & Tan (2018)[a]		
$R_\star$ ($R_\odot$)	$T_\star$ (K)	$L_\star$ (10^3 $L_\odot$)	χ^2
11.2	16,298	7.83	1.89

	Robitaille et al. (2006)[a]		
$R_\star$ ($R_\odot$)	$T_\star$ (K)	$L_\star$ (10^3 $L_\odot$)	χ^2
110.7	4428	4.17	0.81

EGO-12 Sample: Temperature and Mass

- Dust (graybody) and gas (NH_3) temperatures are similar for all sources; clump masses are therefore also similar

- Most sources fall between 22 – 29 K and 100 – 800 Msun; median T = 26 K, similar to ATLASGAL Top100 sample (Giannetti et al. 2014)

- Usually, $T_{NH3} < T_{dust}$ slightly, in agreement with the trends noted for the ATLASGAL Top100 sample in Giannetti et al. (2017), König et al. (2017)

EGO-12 Sample: L/M Ratio

- No trend in L/M with mass
- L/M are typically between 5-60 Lsun/Msun, with median = 24.7+/-8.4, regardless of method used to determine L
- L/M span ~2.5x for a given source, depending on which L is used

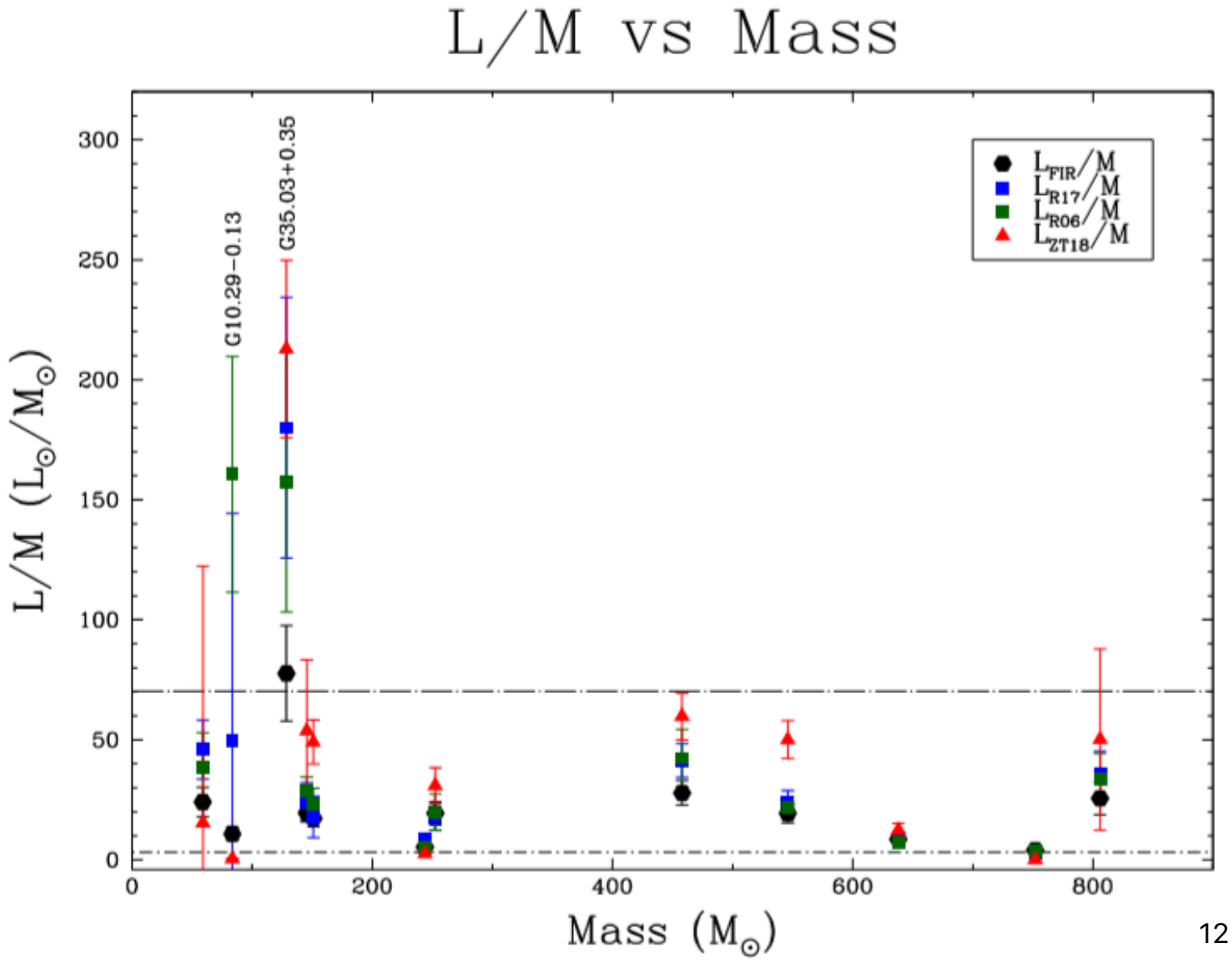

EGO-12 Sample: L/M in Context

- L/M values are comparable to the Carpenter et al. (1990), Elia et al. (2017), Urquart et al. (2018) samples (10x higher than for low- and intermediate-mass-only regions, Enoch et al. 2009)

- L/M ratio is similar, but L and M ~10x lower, than Motte Large Program sample

- Compared to Tigé et al. (2017; *Herschel*-HOBYS program), EGOs span the “IR-quiet” and “IR-bright” flux and L/M values

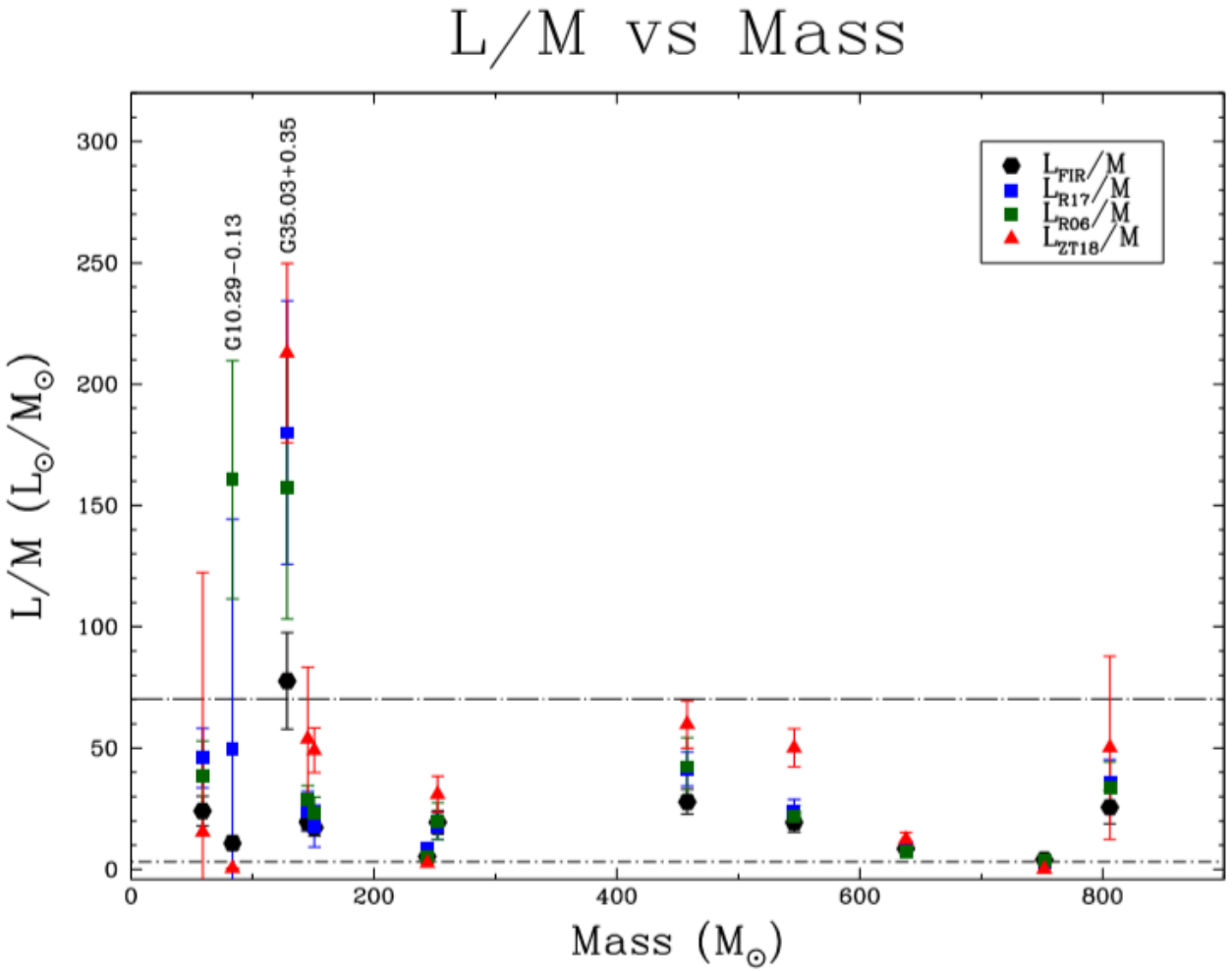

EGO-12 Sample: Transitional Population?

- Compared to ATLASGAL Top100 sample, EGOs span the “IR-weak” and “IR-bright” temperature and flux values (2.6 Jy at 4 kpc), but with some significant scatter in temperature space
- In combination with EGO location in L/M space as compared to other samples, this suggests that it is possible EGOs represent a transitional population of MYSOs

- Caveats:
  - Small sample sizes
  - Sample selection methods for both EGO-12 and Top100 samples

Future Work

Construct radio SEDs to disentangle emission mechanisms (dust, free-free, synchrotron):

- ALMA 1.3 mm and 3.2 mm continuum (~0.8” resolution, ~0.1 mJy/beam)
- JVLA 1.3 cm and 5 cm continuum; H_2O, CH_3OH, and NH_3 (3,3) maser observations (~0.3” resolution, ~10 uJy/beam continuum sensitivity)

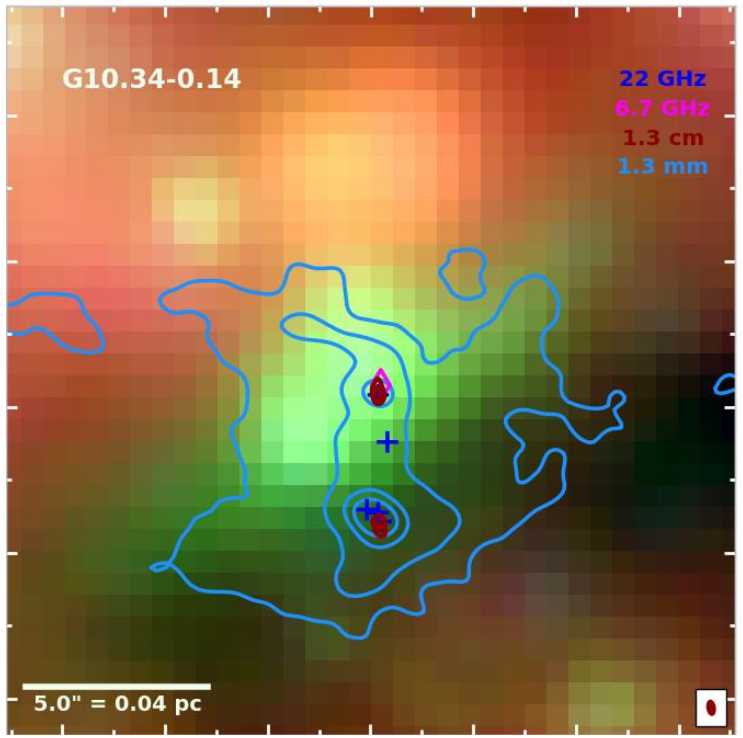

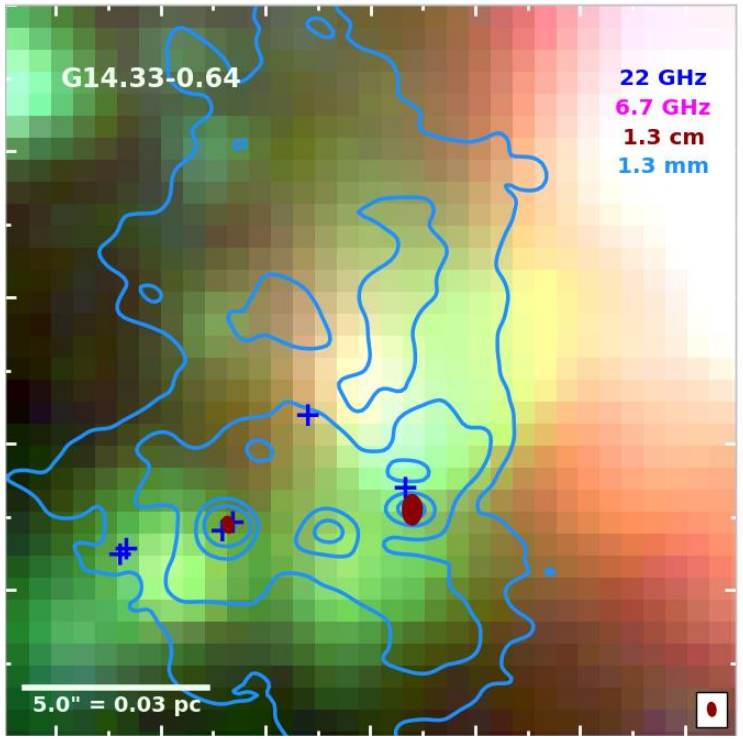

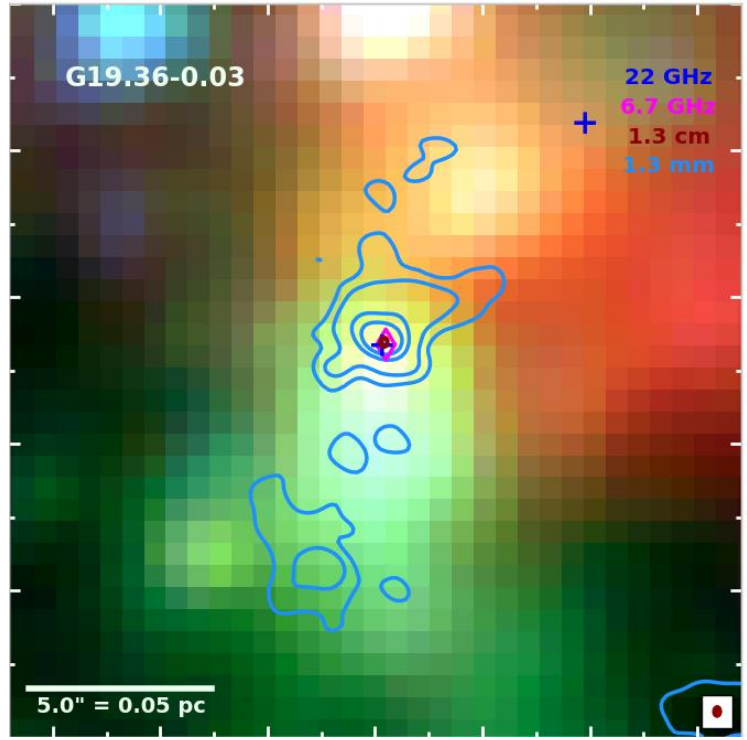

Summary

- Massive-source multiplicity at an angular resolution of ~3.0” is 1-2 per EGO, in line with results published by other teams (e.g. Rosero et al. 2009, SOMA survey)
- Physical properties returned by various radiative-transfer modeling packages can vary significantly, but luminosities are quite consistent regardless of model package
- Temperatures are consistent with those published for similar samples (e.g. Top100 sample, Giannetti et al. 2014, 2017; König 2017)
- L/M values show no trend with mass, and are similar to those published by other teams, even when other samples contain more massive and more luminous sources (e.g. Motte Large Program survey; *Herschel*-HOBYS; Tigé et al. 2017)
- EGO-12 sources lie between “IR-quiet” and “IR-bright” populations identified by other teams in both L/M and temperature space; possible indication that EGOs are a transitional population, but with some caveats

Details of Robitaille et al. (2017) Model Results

Table 10
χ^2 and $P(D|M)$ Scores for Robitaille (2017) Model Sets[a,b]

G10.29−0.13				**G10.34−0.14**[c]				G11.92−0.61			
Model	χ^2	Model	$P(D\|M)$	Model	χ^2	Model	$P(D\|M)$	Model	χ^2	Model	$P(D\|M)$
spubhmi	0.0003	s-u-smi	0.0519	**s-pbhmi**	1.51	**s-pbhmi**	0.0029	s-pbsmi	3.14	s-ubsmi	0.0015
spubsmi	0.002	spu-smi	0.0422	s-pbsmi	2.30	s-pbsmi	0.0028	s-pbhmi	3.69	s-pbsmi	0.0009
s-pbsmi	0.004	spubhmi	0.0408625	spubsmi	6.75	spubhmi	0.0008625	spubsmi	3.87	s-pbhmi	0.0007
s-ubsmi	0.013	s-pbhmi	0.0384	spubhmi	8.53	s-ubsmi	0.0008	spubhmi	4.73	spubsmi	0.000675
s-u-smi	0.017	s-ubhmi	0.0359	s-ubsmi	12.13	s-ubhmi	0.0359	s-ubhmi	5.02	s-ubhmi	0.0006
s-pbhmi	0.022	spubsmi	0.02725	s-ubhmi	15.52	spubsmi	0.0325	s-ubsmi	6.08	spubhmi	0.0004125
s-ubhmi	0.028	s-pbsmi	0.0261	spu-smi	21.70	spu-smi	0	s-u-smi	34.70	spu-smi	0
spu-smi	0.044	s-ubsmi	0.0217	s-u-smi	23.52	s-u-smi	0	spu-smi	40.68	s-u-smi	0
G12.91−0.03				**G14.33−0.64**				G14.63−0.58			
Model	χ^2	Model	$P(D\|M)$	Model	χ^2	Model	$P(D\|M)$	Model	χ^2	Model	$P(D\|M)$
s-pbhmi	1.51	**s-pbhmi**	0.0013	**s-pbsmi**	0.45	**s-pbsmi**	0.0034	s-pbhmi	3.68	s-pbsmi	0.0007
spubhmi	1.84	s-ubsmi	0.0013	s-pbhmi	0.80	s-pbhmi	0.003	s-pbsmi	4.41	s-pbhmi	0.0006
spubsmi	2.84	s-pbsmi	0.0011	spubsmi	2.30	s-ubhmi	0.0006	spubsmi	24.81	spubsmi	0.0001
s-ubsmi	3.03	s-ubhmi	0.0006	spubhmi	4.40	s-ubsmi	0.0006	spubhmi	24.87	spubhmi	0.00005
s-pbsmi	3.99	spubsmi	0.00055	s-ubsmi	4.51	spubhmi	0.000425	s-ubhmi	38.19	s-ubhmi	0
s-ubhmi	4.84	spubhmi	00003375	s-ubhmi	4.94	spubsmi	0.000425	s-ubsmi	47.43	s-ubsmi	0
s-u-smi	28.58	spu-smi	0	spu-smi	12.78	spu-smi	0.0003	spu-smi	67.87	spu-smi	0
spu-smi	31.37	s-u-smi	0	s-u-smi	12.84	s-u-smi	0.0002	s-u-smi	70.85	s-u-smi	0